



## Parallel crack near the interface of magnetoelastic bimetals

Wen-ye Tian <sup>\*</sup>, Ulrich Gabbert

*Fakultät für Maschinenbau, Institut für Mechanik, Universität Magdeburg, Magdeburg 39106, Germany*

### Abstract

A parallel crack near the interface of magnetoelastic bimetals is considered. The crack is modelled by using the continuously distributed edge dislocations, which are described by the density functions defined on the crack line. With the aid of the fundamental solution for the edge dislocation, the present problem is reduced to a system of singular integral equations, which can be numerically solved by using the Chebyshev numerical integration technique. Then, the stress intensity factor (SIF), the magnetic induction intensity factor (MIIF) and the electric displacement intensity factor (EDIF) at the crack tips are evaluated. Using these fracture criteria, the cracking behaviour of magnetoelastic bimetals is investigated. Numerical examples demonstrate that the interface, mechanical load, magnetic load and material mismatch condition are all important factors affecting the fracture toughness of the magnetoelastic bimetals.

© 2004 Elsevier B.V. All rights reserved.

PACS: 82.45.Un; 46.15.-x; 46.50.+a

Keywords: Magnetoelastic bimetal; Interface; Crack; Edge dislocation

### 1. Introduction

Nowadays, the crack/inclusion-like defect problems in magnetoelastic solids are attracting more and more attention. For example, Huang and Kuo [1] investigated the inclusion problems encountered in magnetoelastic media with

the aid of the three-dimensional magnetoelastic Green's function. Liu et al. [2] proposed the Green's functions for anisotropic magnetoelastic solids with an elliptical cavity or a crack. Sih and Song [3] considered the magnetic and electric poling effects associated with crack growth in one kind of magnetoelastic composite materials namely  $\text{BaTiO}_3\text{-CoFe}_2\text{O}_4$ . These achievements mainly considered the crack/inclusion-related problems in homogeneous magnetoelastic bodies. Little work has been done

<sup>\*</sup> Corresponding author.

E-mail address: [tianwenye@hotmail.com](mailto:tianwenye@hotmail.com) (W.-y. Tian).

on analysing similar problems in magneto-electroelastic bimaterial solids. Studying of the interface-crack interaction problems in magento-electroelastic bimaterials becomes more and more important from a theoretical as well as from practical point of view, due to for example, bonding of different smart materials widely used in industry, where manufacturing imperfections in bonding usually appear as cracks near the bonded interface [4–6]. On the other hand, since the dislocation analysis has been recognized as a favoured tool for analysing the fracture problems in various kinds of smart materials [6], it will be adopted again in this paper to simulate the crack residing in magneto-electroelastic media.

**2. A dislocation in two bonded magneto-electroelastic half-planes**

For a two dimensional linear magneto-electroelastic medium problem, the magneto-electroelastic field can be represented in terms of five functions  $f_1(z_1), f_2(z_2), f_3(z_3), f_4(z_4)$  and  $f_5(z_5)$  [2]. Each of them is holomorphic in its argument. With these holomorphic functions (or complex potentials), the general solutions for displacements  $u_1, u_2$  and  $u_3$ , electric potential  $\varphi$ , magnetic potential  $\phi$ , stresses  $\sigma_{11}, \sigma_{12}, \sigma_{13}, \sigma_{21}, \sigma_{22}$  and  $\sigma_{23}$ , electric displacements  $D_1$  and  $D_2$ , and magnetic inductions  $B_1$  and  $D_2$  could be expressed as

$$\begin{aligned} \{u_i\} &= 2\text{Re} \left[ \sum_{j=1}^5 A_{ij} f_j(z_j) \right] \\ \{\sigma_{2i}\} &= 2\text{Re} \left[ \sum_{j=1}^5 L_{ij} f'_j(z_j) \right] \\ \{\sigma_{1i}\} &= -2\text{Re} \left[ \sum_{j=1}^5 L_{ij} \mu_j f'_j(z_j) \right], \end{aligned} \tag{1}$$

where  $\{u_i\} = \{u_1, u_2, u_3, \varphi, \phi\}$ ,  $\{\sigma_{1i}\} = \{\sigma_{11}, \sigma_{12}, \sigma_{13}, D_1, B_1\}$ ,  $\{\sigma_{2i}\} = \{\sigma_{21}, \sigma_{22}, \sigma_{23}, D_2, B_2\}$ . The prime ( ' ) denotes differentiation with respect to the associated arguments, and  $\mathbf{A}$  and  $\mathbf{L}$  are two  $5 \times 5$  matrices depending on material constants [2]. Consider an infinite magneto-electroelastic bimaterial body with materials 1 and 2, respectively occupy-

ing the upper and lower half planes. Assume there exists a near-interface dislocation singularity in material 2 (see Fig. 1). As Miller [4] and Tian et al. [6] did, define a new set of potentials  $\Pi_k$  in terms of the  $f'_j$  for the lower half plane and the  $f'^U_j$  for the upper half plane as

$$\mathbf{\Pi}(z) = \begin{bmatrix} \mathbf{A} & -\overline{\mathbf{A}^U} \\ \mathbf{L} & -\overline{\mathbf{L}^U} \end{bmatrix} \begin{bmatrix} \mathbf{f}'(z) \\ \overline{\mathbf{f}'^U(z)} \end{bmatrix} \quad (\text{Im}\{z\} < 0) \tag{2}$$

$$\mathbf{\Pi}(z) = \begin{bmatrix} \mathbf{A}^U & -\overline{\mathbf{A}} \\ \mathbf{L}^U & -\overline{\mathbf{L}} \end{bmatrix} \begin{bmatrix} \mathbf{f}'^U(z) \\ \overline{\mathbf{f}'(z)} \end{bmatrix} \quad (\text{Im}\{z\} > 0) \tag{3}$$

where  $\mathbf{\Pi}(z) = \{\Pi_1(z), \Pi_2(z), \dots, \Pi_{10}(z)\}$ . The superscript 'U' indicates the upper half plane and the over bar denotes complex conjugation. Now, the jump in each of the physical quantities required to be continuous across the interface is given by a simple relation of the form  $\Pi_k^+(x) - \Pi_k^-(x)$ .

Consider a complex potential corresponding to the basic singular solution for plane magneto-electroelastic body, which allows the modeling of concentrated forces, electric displacements, magnetic inductions, displacements, electric potentials and magnetic potentials [4,6]

$$f'_j(z) = \frac{\rho_j}{z - z_{0j}} \tag{4}$$

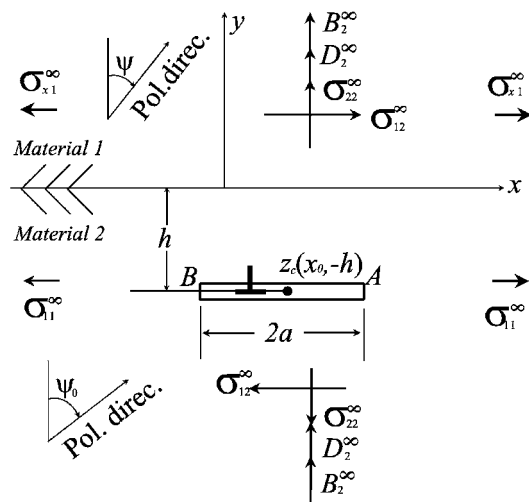


Fig. 1. An edge dislocation and a parallel crack near interface.

in which  $z_{0j} = x_0 + \mu_j y_0$ , with  $x_0$  and  $y_0$  locating the singularity. The net physical quantity jumps induced by the singularities are as follows:

$$\operatorname{Im} \sum_{j=1}^5 L_{ij} \rho_j = -\frac{X_i}{4\pi} \quad (i = 1, 2, \dots, 5) \quad (5)$$

$$\operatorname{Im} \sum_{j=1}^5 A_{ij} \rho_j = -\frac{\Delta u_i}{4\pi} \quad (i = 1, 2, \dots, 5).$$

The quantities  $X_1, X_2, X_3, X_4$  and  $X_5$  represent the net forces, the net electric displacement and the net magnetic induction on any contour encircling the singularity, and  $\Delta u_1, \Delta u_2, \Delta u_3, \Delta u_4$  and  $\Delta u_5$  are the displacements, the electric potential and the magnetic potential jumps, respectively. In the case of a pure dislocation singularity,  $X_i (i = 1, 2, \dots, 5)$  are taken to be zero. Then, by substituting Eq. (4) into Eqs. (2) and (3), the potentials  $\Pi$  corresponding to the  $f'_j$  in Eq. (4) can be obtained directly. Provided the singularity locates in the lower half plane and  $f_j^U = 0$ , then

$$\Pi_k(z) = \sum_{j=1}^5 \varpi_{kj} \frac{\rho_j}{z - z_{0j}} \quad (\operatorname{Im}\{z\} < 0) \quad (6)$$

$$\Pi_k(z) = \sum_{j=1}^5 -\bar{\varpi}_{kj} \frac{\bar{\rho}_j}{z - \bar{z}_{0j}} \quad (\operatorname{Im}\{z\} > 0),$$

where

$$\begin{aligned} \varpi_{1j} &= A_{1j}, & \varpi_{2j} &= A_{2j}, & \varpi_{3j} &= A_{3j}, & \varpi_{4j} &= A_{4j}, \\ \varpi_{5j} &= A_{5j}, \\ \varpi_{6j} &= L_{1j}, & \varpi_{7j} &= L_{2j}, & \varpi_{8j} &= L_{3j}, & \varpi_{9j} &= L_{4j}, \\ \varpi_{10j} &= L_{5j}. \end{aligned} \quad (7)$$

From Eq. (6), it is easily found that  $\Pi_k^+(x) - \Pi_k^-(x) \neq 0$ , which means that the interface condition is not satisfied, i.e. the tractions, displacements, electric displacement, electric field, magnetic induction and magnetic field are not continuous across the interface. In order to satisfy the interface condition, the following additional potentials are further introduced:

$$\hat{\Pi}_k(z) = \sum_{j=1}^5 -\bar{\varpi}_{kj} \frac{\bar{\rho}_j}{z - \bar{z}_{0j}} \quad (\operatorname{Im}\{z\} < 0) \quad (8)$$

$$\hat{\Pi}_k(z) = \sum_{j=1}^5 \varpi_{kj} \frac{\rho_j}{z - z_{0j}} \quad (\operatorname{Im}\{z\} > 0).$$

The sum of the potentials in Eqs. (6) and (8) now satisfies the interface condition. The potentials  $\Pi_k$  can be finally expressed as

$$\Pi_k(z) = \sum_{j=1}^5 \left[ \varpi_{kj} \frac{\rho_j}{z - z_{0j}} - \bar{\varpi}_{kj} \frac{\bar{\rho}_j}{z - \bar{z}_{0j}} \right]. \quad (9)$$

Using the relation (2), the complex potentials  $f'$  can be expressed in terms of  $\Pi$  as follows

$$\begin{aligned} f'_j(z) &= m_{jk} \Pi_k(z) \\ \overline{f'_j(z)} &= -\bar{m}_{jk} \Pi_k(\bar{z}) \quad (\operatorname{Im}\{z\} < 0), \end{aligned} \quad (10)$$

where  $m_{jk}$  are the components of the inverse of the matrix in Eq. (2). Hence, the potentials  $f'_j$  used for modelling the dislocation singularity are

$$f'_j(z_j) = \frac{\rho_j}{z_j - z_{0j}} - \sum_{k=1}^{10} m_{jk} \sum_{l=1}^5 \bar{\varpi}_{kl} \frac{\bar{\rho}_l}{z_j - \bar{z}_{0l}}. \quad (11)$$

### 3. Singular integral equations

Now, the dislocation solution of Eq. (11) can be used to model the near interface crack. Consider an infinite bimaterial body containing a parallel crack AB near the interface, as shown in Fig. 1, where  $h$  indicates the distance between the crack and the interface and  $z_c(x_0, -h)$  is the center of the crack. If the crack line is defined by  $z = z_c + \xi$ , then the  $\rho_j$  in Eq. (11) should be substituted by functions  $\rho_j(\xi)$ . The corresponding potentials will be given by integrals of the  $\rho_j(\xi)$  along the crack

$$\begin{aligned} f'_j(z_j) &= \int_{-a}^a \frac{\rho_j(\xi) d\xi}{z_j - z_{0j}(\xi)} - \sum_{k=1}^{10} m_{jk} \sum_{l=1}^5 \bar{\varpi}_{kl} \\ &\quad \times \int_{-a}^a \frac{\bar{\rho}_l(\xi) d\xi}{z_j - \bar{z}_{0l}(\xi)}. \end{aligned} \quad (12)$$

Then, using Eqs. (1) and (12), the stress, electric and magnetic field at any point  $z$  due to the near-interface crack can be evaluated. According to the free condition of the traction, charge and electric current on crack faces, the stresses, electric displacement and magnetic induction acting on the crack surface must be balanced by the resultant stresses, electric displacement and magnetic induction applied on the crack surface. This free

condition leads to the following singular integral equation [4,6]:

$$2Re \sum_{j=1}^5 \left\{ L_{ij} \left[ \int_{-a}^a \frac{\rho_j(\xi) d\xi}{\zeta - \xi} - \sum_{k=1}^{10} m_{jk} \right. \right. \\ \left. \left. \times \sum_{l=1}^5 \bar{w}_{kl} \int_{-a}^a \frac{\bar{\rho}_l(\xi) d\xi}{\zeta - \xi - (\mu_j - \bar{\mu}_l)h} \right] \right\} = g_i(\zeta), \quad (13)$$

where  $|\xi| < a$ ,  $|\zeta| < a$ ,  $g_i(\zeta) = \{q(\zeta), p(\zeta), 0, d(\zeta), b(\zeta)\}$ , the functions  $q(\zeta)$  and  $p(\zeta)$  are the known tractions,  $d(\zeta)$  the known electric displacement and  $b(\zeta)$  the known magnetic induction due to the applied load. By using the Chebyshev numerical integration and the Chebyshev polynomial techniques, the integral Eq. (13) can be numerically solved readily. In terms of the first kind of the Chebyshev polynomial,  $\rho_j(\xi)$  is expressed as

$$\rho_j(\xi) = \frac{1}{\sqrt{1-t^2}} \sum_{l=0}^N A_{jl} T_l(t) \quad (t = \xi/a), \quad (14)$$

where  $T_l(t)$  are the Chebyshev polynomials of the first kind,  $A_{jl}$  the coefficients of the Chebyshev polynomials and  $N$  is the number of Gauss–Chebyshev collocation points. Once the Eq. (13) has been solved, the intensity factors at the crack tips can be evaluated by using the following formula [5]

$$K_i = \sqrt{\pi a} \left\{ \pm 2\pi Re \sum_{j=1}^5 \left[ L_{ij} \sum_{l=0}^N A_{jl} T_l(\pm 1) \right] \right\}, \quad (15)$$

where in  $K_i = \{K_{II}, K_I, K_{III}, K_e, K_m\}$ , the subscripts I, II, and III refer to the Mode I, Mode II and Mode III SIFs,  $e$  regards the EDIF and  $m$  the MIF, and the quantities with positive and negative signs denote the right and the left tips of the crack, respectively.

#### 4. Numerical results and discussion

Herein, a special magnetoelastic bimaterial is considered. Both its upper and lower half-plane materials are the same kind of material BaTiO<sub>3</sub>–CoFe<sub>2</sub>O<sub>4</sub> [3,7] but with different magnetic-electric poling directions. The quantities  $\psi$  and  $\psi_0$  indicate the poling directions of the upper

and the lower half-plane materials with respect to the axis  $y$  (see Fig. 1). Assume the volume fraction for BaTiO<sub>3</sub> in BaTiO<sub>3</sub>–CoFe<sub>2</sub>O<sub>4</sub> composite is  $V_f = 0.5$ . The material parameters are given in Appendix A. In the following calculations, same mechanical load, i.e.  $\sigma_{22}^\infty = \sigma_{11}^\infty = 4 \times 10^6 \text{ N/m}^2$ ,  $\sigma_{12}^\infty = 0$  and  $\sigma_{x1}^\infty \neq 0$ , is considered, and take  $\psi_0 = 0$ . Let  $h/a = 0.3$ . The normalized Mode I SIF  $K_I^A/K_0$  ( $K_0 = \sqrt{\pi a \sigma_{22}^\infty}$ ) at crack tip A was calculated under different loading conditions. Its varying tendencies with the increasing angle  $\psi$  are plotted in Fig. 2, where, Fig. 2(a) is for  $D_2^\infty = 0$  and (b) for  $D_2^\infty = 1 \times 10^{-4} \text{ C/m}^2$ . From Fig. 2(a) and (b), it is found that under the loading conditions considered, the  $K_I^A/K_0$  increases first with the increasing angle  $\psi$  until up to the maximum value, which indicates the maximum amplification effect. The  $\psi$  corresponding to the maximum amplification effect is called the maximum amplification angle. Then, the  $K_I^A/K_0$  drops down until the minimum value is reached, which indicates the maximum shielding effect. The corresponding value of  $\psi$ , when  $K_I^A/K_0 = 1$ , is called the neutral shielding angle, at which the interface-crack interaction effect transforms from the amplification region to the shielding region. The  $\psi$  at which the maximum shielding effect takes place is called the maximum shielding angle. From this angle, the  $K_I^A/K_0$  increases again with the increasing  $\psi$ . It is noticed that, when  $\psi = 0^\circ$  or  $360^\circ$ , i.e. in homogeneous case, the magnetic load takes no effect on the  $K_I^A/K_0$  (i.e.  $K_I^A/K_0 = 1$ ) whether the electric load is considered or not. This phenomenon coincides with the conclusion found by Wang and Mai [8]. However, when the interface exists (i.e.  $\psi \neq 0^\circ$  or  $360^\circ$ ), the magnetic loading takes a significant effect on the  $K_I^A/K_0$ . It not only shifts the maximum amplification angle, the neutral shielding angle and the maximum shielding angle, but also changes the magnitudes of the maximum amplification effect and the maximum shielding effect. The comparison of Fig. 2(a) and (b) shows that both the maximum amplification angle and the maximum shielding angle are changed after the positive electric loading is introduced. This indicates that the mechanical load, the electric load and the magnetic load are coupled together to take effect on the  $K_I^A/K_0$  when the interface exists.

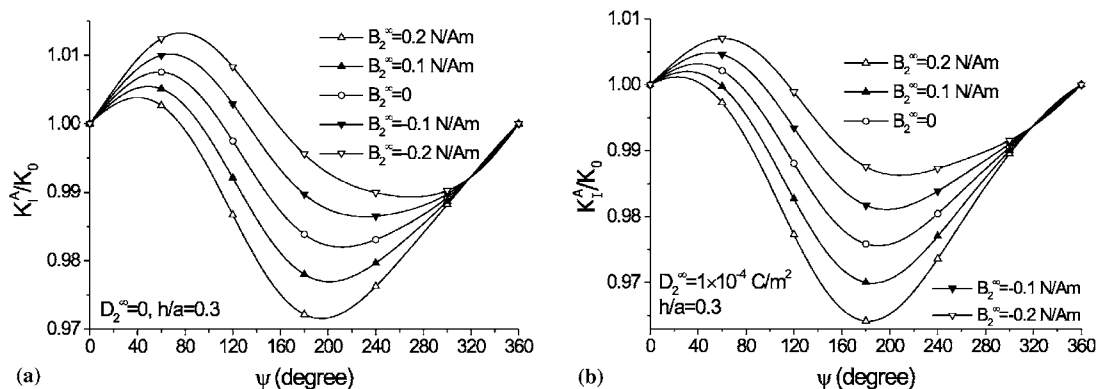


Fig. 2.  $K_I^A/K_0$  vs the angle  $\psi$ .

Moreover, it is seen that the positive and negative magnetic loading play an opposite role on the  $K_I^A/K_0$ , i.e. the positive magnetic loading impedes the maximum amplification effect and aids the maximum shielding effect, while the negative magnetic loading aids the maximum amplification effect and impedes the maximum shielding effect. The most interesting is that the curves derived under different magnetic loading conditions intersect with each other at one point when  $\psi = 319.02^\circ$  whether the electric loading  $D_2^\infty$  is considered or not. This implies that at this special angle, neither the positive nor the negative magnetic loading takes effect on the  $K_I^A/K_0$ . We call this special angle the neutral magnetic loading angle.

Let  $D_2^\infty = 1 \times 10^{-4} \text{ C/m}^2$ . The normalized EDIF  $K_e^A/K_0^e$  ( $K_0^e = \sqrt{\pi a} \times 10^{-4} \text{ C/m}^2$ ) derived under dif-

ferent magnetic loading conditions are shown in Fig. 3(a). The calculation results disclose that a neutral magnetic loading angle  $\psi = 328.5^\circ$  also exists in Fig. 3(a), though it cannot be easily identified from the figure. It is clearly seen from this figure that the positive and negative magnetic loadings play an opposite role on the  $K_e^A/K_0^e$ . For example, when  $0^\circ < \psi < 328.5^\circ$ , the positive magnetic loading decreases the  $K_e^A/K_0^e$ , while the negative magnetic loading increases it. In homogeneous case, i.e. when  $\psi = 0^\circ$  or  $360^\circ$ , neither the positive nor the negative magnetic loading takes effect on the  $K_e^A/K_0^e$ . Let  $D_2^\infty = 0$ . The normalized MIIF  $K_m^A/K_0^m$  ( $K_0^m = \sqrt{\pi a} \times 0.1 \text{ N/Am}$ ) derived under different magnetic loading conditions are shown in Fig. 3(b). From Fig. 3(b), the aiding effect of the positive magnetic loading and the impeding effect

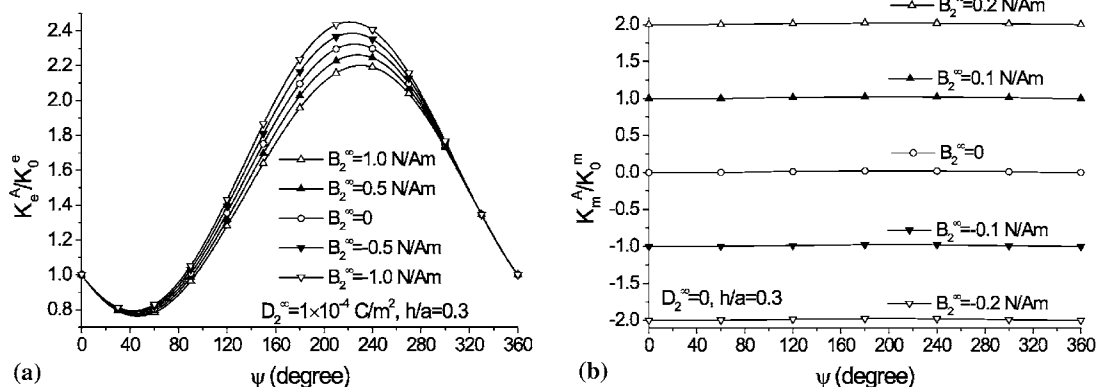


Fig. 3.  $K_e^A/K_0^e$  and  $K_m^A/K_0^m$  vs the angle  $\psi$ .

of the negative magnetic loading on the  $K_m^A/K_0^m$  can be easily found whether in homogeneous ( $\psi = 0^\circ$  or  $360^\circ$ ) or dissimilar ( $\psi \neq 0^\circ$  or  $360^\circ$ ) case.

## 5. Concluding remarks

The research reveals that the interface, mechanical load, magnetic load and material mismatch condition are all important factors affecting the fracture toughness of the magnetoelastic bimaterial. Distinctly different from the conclusion found in homogeneous case [8], the positive and negative magnetic loads play an opposite role in the cracking behaviour of magnetoelastic bimaterial. The fracture toughness of the magnetoelastic bimaterial is reduced or increased depending on the direction of the applied magnetic field.

## Acknowledgment

The work presented in the paper was fully supported by the Alexander von Humboldt Foundation (Germany).

## Appendix A

The elastic stiffness constants:  $C_{11} = 226$  GPa,  $C_{12} = 125$  GPa,  $C_{13} = 124$  GPa,  $C_{33} = 216$  GPa,  $C_{44} = 44$  GPa, the piezoelectric constants:  $e_{31} =$

$-2.2$  C/m<sup>2</sup>,  $e_{33} = 9.3$  C/m<sup>2</sup>,  $e_{15} = 5.8$  C/m<sup>2</sup>, the piezomagnetic constants:  $h_{31} = 290.2$  N/Am,  $h_{33} = 350$  N/Am,  $h_{15} = 275$  N/Am, the dielectric permittivities:  $\omega_{11} = 56.4 \times 10^{-10}$  C<sup>2</sup>/Nm<sup>2</sup>,  $\omega_{33} = 63.5 \times 10^{-10}$  C<sup>2</sup>/Nm<sup>2</sup>, the magnetic permeabilities:  $\alpha_{11} = 297 \times 10^{-6}$  Ns<sup>2</sup>/C<sup>2</sup>,  $\alpha_{33} = 83.5 \times 10^{-6}$  Ns<sup>2</sup>/C<sup>2</sup>, and the electromagnetic constants:  $\gamma_{11} = 5.367 \times 10^{-12}$  Ns/VC,  $\gamma_{33} = 2737.5 \times 10^{-12}$  Ns/VC.

## References

- [1] J.H. Huang, W.S. Kuo, The analysis of piezoelectric/piezomagnetic composite materials containing an ellipsoidal inclusion, *J. Appl. Phys.* 81 (3) (1997) 1378–1386.
- [2] J.X. Liu, X.L. Liu, Y.B. Zhao, Green's functions for anisotropic magnetoelastic solids with an elliptical cavity or a crack, *Int. J. Eng. Sci.* 39 (2001) 1405–1418.
- [3] G.C. Sih, Z.F. Song, Magnetic and electric poling effects associated with crack growth in BaTiO<sub>3</sub>-CoFe<sub>2</sub>O<sub>4</sub> composite, *Theor. Appl. Fract. Mech.* 39 (2003) 209–227.
- [4] G.R. Miller, Analysis of cracks near interfaces between dissimilar anisotropic materials, *Int. J. Eng. Sci.* 27 (1989) 667–678.
- [5] X.L. Han, F. Ellyin, Z.H. Xia, Interaction among interface, multiple cracks and dislocations, *Int. J. Solids Struct.* 39 (2002) 1575–1590.
- [6] W.Y. Tian, K.T. Chau, Arbitrarily oriented crack near interface in piezoelectric bimaterials, *Int. J. Solids Struct.* 40 (2003) 1943–1958.
- [7] J.Y. Li, Magnetoelastic multi-inclusion and inhomogeneity problems and their applications in composite materials, *Int. J. Eng. Sci.* 38 (2000) 1993–2011.
- [8] B.L. Wang, Y.W. Mai, Crack tip field in piezoelectric/piezomagnetic media, *Eur. J. Mech. A Solids* 22 (2003) 591–602.